

ON THE GROUND-STATE ENERGY OF A MIXTURE OF TWO DIFFERENT OPPOSITELY POLARIZED FERMIONIC GASES

PIOTR CHANKOWSKI[†], JACEK WOJTKIEWICZ[‡]

Faculty of Physics, University of Warsaw
Pasteura 5, 02-093 Warszawa, Poland

*Received 23 December 2021, accepted 31 December 2021,
published online 16 January 2022*

We report on the results of the computation of the order of $(k_F a_0)^2$ correction, where $k_F = 3\pi^2 \rho$ is the Fermi wave vector and a_0 the s -wave scattering length of the repulsive interaction, to the ground-state energy of a mixture of oppositely polarized N_a spin-1/2 fermions a of masses m_a and N_b spin-1/2 fermions b of masses m_b ($\rho = N/V$, $N = N_a + N_b$). It is shown that the results of the paper in which the same correction has been computed entirely numerically, using a more traditional approach, can be easily and semianalytically reproduced using the effective field theory technique.

DOI:10.5506/APhysPolB.53.1-A3

1. Introduction

Whether the ferromagnetic behaviour of a gas of spin-1/2 fermions (*i.e.* the emergence of the so-called itinerant ferromagnetism) can be induced by their repulsive spin-independent interaction is experimentally still an open issue which is being studied by exploiting the upper branch of the Feshbach resonance allowing to appropriately tune the interaction strength of fermionic atoms of ultra-cold gases [2, 3]. Theoretical studies of this problem have a long history. The classic mean-field calculation [4] predicts that the critical interaction strength above which the ground-state energy E_Ω of the polarized gas of spin-1/2 fermions is lower than that of the nonpolarized one is $k_F a_0 = \pi/2$, where $k_F = 3\pi^2 N/V$ is the gas Fermi vector and a_0 is the s -wave scattering length characterizing the repulsive interaction. More recently, computations of the ground-state energy going beyond the mean-field approximation [5], also ones exploiting the quantum Monte Carlo

[†] chank@fuw.edu.pl

[‡] wjacek@fuw.edu.pl

simulations [6], have resulted in a lower critical value, $k_F a_0 \approx 0.8$. This relatively large critical interaction strength seems to be a source of considerable difficulties in experimental observation of the effect [3, 7].

Among different possible ways of favouring the appearance of ferromagnetism the use of a mixture of oppositely polarized different fermionic atomic gases (of different masses) has been proposed. The computation of the ground-state energy of such a mixture in the approximation going one order beyond the simple mean-field one, *i.e.* up to terms of the order of $(k_F a_0)^2$ has been undertaken in [1] and a variety of possible phases of the system has been exhibited by a detailed numerical study.

The order $(k_F a_0)^2$ correction in the perturbative expansion of the ground-state energy E_Ω of the interacting fermionic system can be computed either more traditionally, as in [1], by the method outlined in [8] which leads to rather complicated multiple integrals which must be evaluated numerically, or using the effective theory [9] (see also [10, 11] for applications of this method to many-body systems). The latter method is particularly well suited for the case in which the interaction potential is not given explicitly but is from the outset characterized only by the set of scattering lengths a_ℓ and effective radii r_ℓ , $\ell = 0, 1, \dots$. It allowed to easily recover [9] the classic order $(k_F a_0)^2$ result in the case of an unpolarized gas of identical fermions of arbitrary spin and to extend it up to yet higher orders [9, 12]. Very recently, we have used it [13] to obtain the order $(k_F a_0)^2$ correction to the ground-state energy of the diluted polarized gas of identical spin-1/2 fermions, easily numerically recovering (and thereby demonstrating its universality) the old analytic result of Kanno [14] which has been obtained by the method of [8] for the specific hard-core interaction potential.

It is a natural step to extend the effective theory approach to the case of a diluted mixture of oppositely polarized fermions of different masses. We present this extension in this paper. It turns out that it reduces to only a small modification of the computation done in [13] and as there, part of the computations can be done analytically; the remaining integrals are simple (compared to the ones done in [1]) and can be easily evaluated numerically with the help of a three-line `Mathematica` code using its standard built-in integration routines. Moreover, the correctness of the computation is partially controlled by the cancellation of ultraviolet divergences. The computation is sketched in Section 2 and the comparison and the discussion are given in Section 3.

2. Computation

We consider a mixture of N_a spin-1/2 (nonrelativistic) fermions of masses m_a (a -fermions), all having spins up and N_b spin-1/2 fermions of masses m_b having spins down (b -fermions), enclosed in a box of volume V and

interacting with one another through a spin-independent two-body short range repulsive potential. In the traditional language of quantum mechanics, the Hamiltonian H of the system is of the form of

$$\begin{aligned}
 H = & -\frac{\hbar^2}{2m_a} \sum_{i_a=1}^{N_a} \nabla_{i_a}^2 - \frac{\hbar^2}{2m_b} \sum_{i_b=1}^{N_b} \nabla_{i_b}^2 + \sum_{i_a, i_b} V_{\text{pot}}(|\mathbf{r}_{i_a} - \mathbf{r}_{i_b}|) \\
 & + \frac{1}{2} \sum_{i_a \neq j_a} V_{\text{pot}}(|\mathbf{r}_{i_a} - \mathbf{r}_{j_a}|) + \frac{1}{2} \sum_{i_b \neq j_b} V_{\text{pot}}(|\mathbf{r}_{i_b} - \mathbf{r}_{j_b}|), \quad (1)
 \end{aligned}$$

where $V_{\text{pot}}(|\mathbf{r}|)$ is a repulsive, spin-independent interaction potential and the wave function ψ of the system, satisfying periodic boundary conditions in the box of volume $V = L \times L \times L$ should be properly antisymmetrized in its N_a arguments $(\mathbf{r}_{i_a}, s_{i_a})$ and in its N_b arguments $(\mathbf{r}_{i_b}, s_{i_b})$, $s_{i_{a/b}} = \pm \frac{1}{2}$. In the rest of the paper, the more convenient formalism of the second quantization is used. Without loss of generality, we assume that $N_a \geq N_b$ (the ratio m_b/m_a can be arbitrary).

If the gas of fermions is diluted, so that the Fermi wave vector $k_F = (3\pi^2 N/V)^{1/3}$ (where $N = N_a + N_b$) is sufficiently small, its ground-state energy E_Ω can be computed using the effective theory approach [9]. As follows from the analysis done there, to obtain E_Ω up to the order $(k_F a_0)^2$, it is sufficient to restrict oneself to the lowest dimension interaction operator, *i.e.* to consider the Hamiltonian of the form of¹

$$\begin{aligned}
 H_{\text{eff}} = H_0 + V_{\text{int}} = & \sum_{\mathbf{p}} \left(\frac{\hbar^2 \mathbf{p}^2}{2m_a} a_{\mathbf{p}}^\dagger a_{\mathbf{p}} + \frac{\hbar^2 \mathbf{p}^2}{2m_b} b_{\mathbf{p}}^\dagger b_{\mathbf{p}} \right) \\
 & + \frac{C_0}{V} \sum_{\mathbf{q}} \sum_{\mathbf{p}_1, \mathbf{p}_2} a_{\mathbf{p}_1 + \mathbf{q}}^\dagger a_{\mathbf{p}_1} b_{\mathbf{p}_2 - \mathbf{q}}^\dagger b_{\mathbf{p}_2}, \quad (2)
 \end{aligned}$$

(the most general effective Hamiltonian has, in principle, infinitely many operator structures of growing dimension [9–11]). In contrast to the underlying “fundamental” Hamiltonian (1), the effective one, (2), is strictly local. The zeroth and first-order contributions to E_Ω

$$E_\Omega^{(0)} + E_\Omega^{(1)} = \frac{V}{6\pi^2} \frac{3}{5} \frac{\hbar^2}{2} \left(\frac{p_{Fa}^5}{m_a} + \frac{p_{Fb}^5}{m_b} \right) + VC_0 \frac{p_{Fa}^3}{6\pi^2} \frac{p_{Fb}^3}{6\pi^2}, \quad (3)$$

¹ Since in the considered system, there are no a -fermions with spin down (b -fermions with spin up), the possible interactions of a -fermions (b -fermions) between themselves do not play any role in determination of E_Ω owing to the Pauli exclusion principle and the nonrelativistic character of the theory (impossibility of particle–antiparticle pair creation) and can, therefore, be omitted.

in which $p_{F_{a/b}} = (6\pi^2 N_{a/b}/V)^{1/3}$ are the Fermi wave-vectors of the a - and b -fermions, can be then immediately obtained by applying to the Hamiltonian (2) the ordinary Rayleigh–Schrödinger expansion in conjunction with the standard methods of second quantization [16, 17]. The coefficient C_0 has to be related to the s -wave scattering length a_0 which is extracted from the expansion ($k = |\mathbf{k}|$)

$$f(k, \theta) = -a_0 \left[1 - ia_0 k + \left(\frac{1}{2} a_0 r_0 - a_0^2 \right) k^2 + \dots \right] - a_1^3 k^2 \cos \theta + \dots \quad (4)$$

of the amplitude of the elastic scattering of the a - and b -fermions with the wave vectors $\mathbf{k}_a = \mathbf{k}$ and $\mathbf{k}_b = -\mathbf{k}$ generated by the interaction V_{int} of (2). The amplitude $f(k, \theta)$ can, in turn, be obtained from the corresponding S-matrix element $S_{\beta\alpha}$ computed in the second quantization formalism with the help of the standard formula [18]

$$\begin{aligned} S_{\beta\alpha} &= \langle \mathbf{k}'_a, \mathbf{k}'_b | \text{T exp} \left(-\frac{i}{\hbar} \int_{-\infty}^{\infty} dt V_{\text{int}}^I(t) \right) | \mathbf{k}_a, \mathbf{k}_b \rangle \\ &\equiv \delta_{\beta\alpha} - \frac{i}{\hbar} (2\pi)^4 \delta^{(4)}(k'_a + k'_b - k_a - k_b) \mathcal{A}, \end{aligned} \quad (5)$$

in which $V_{\text{int}}^I(t)$ is the interaction picture counterpart of the interaction term of (2) written in the continuum normalization

$$\begin{aligned} V_{\text{int}}^I(t) &= C_0 \int d^3\mathbf{x} \psi_a^\dagger(t, \mathbf{x}) \psi_a(t, \mathbf{x}) \psi_b^\dagger(t, \mathbf{x}) \psi_b(t, \mathbf{x}), \\ \psi_a(t, \mathbf{x}) &= \int \frac{d^3\mathbf{k}}{(2\pi)^3} e^{-i\omega_{\mathbf{k}}^a t + i\mathbf{k}\cdot\mathbf{x}} a(\mathbf{k}), \end{aligned} \quad (6)$$

etc., and T is the symbol of the chronological ordering; employed is also the “four-vector” notation in which $k_{a/b}^0 = \omega_{\mathbf{k}}^{a/b} \equiv \hbar\mathbf{k}^2/2m_{a/b}$. The necessary rule is

$$f(k, \theta) = -\frac{m_{\text{red}}}{2\pi\hbar^2} \mathcal{A}(k, \theta), \quad (7)$$

where $m_{\text{red}} \equiv m_a m_b / (m_a + m_b)$ is the reduced mass of the interacting fermions. In the lowest order of the Dyson expansion of (5), one readily finds (see *e.g.* [9, 10]) that $C_0 = (2\pi\hbar^2/m_{\text{red}})a_0$. This allows to express (3) — the first nontrivial approximation to the ground-state energy — in terms of a physical quantity a_0 .

The local character of the interaction term of the Hamiltonian (2) results in ultraviolet divergences in higher-order corrections, both to the scattering amplitude \mathcal{A} extracted from (5) and to E_Ω ; the corrections to the result (3) can be most conveniently computed using the formula²

$$\lim_{T \rightarrow \infty} \exp\left(\frac{-iT(E_\Omega - E_{\Omega_0})}{\hbar}\right) = \lim_{T \rightarrow \infty} \langle \Omega_0 | \text{T exp} \left(-\frac{i}{\hbar} \int_{-T/2}^{T/2} dt V_{\text{int}}^I(t) \right) | \Omega_0 \rangle \quad (8)$$

according to which $(E_\Omega - E_{\Omega_0})/V$ is directly given by $i\hbar$ times the sum of the momentum space connected vacuum Feynman diagrams (the factor $(2\pi)^4 \delta^{(4)}(0)$ arising in evaluating connected vacuum diagrams in the position space is interpreted as VT). The divergences, if regularized in the same way in evaluating formulae (5) and (8), disappear from the result for E_Ω when C_0 and coefficients of other operator structures of the effective Hamiltonian are in it consistently, order by order, traded for the scattering lengths a_ℓ and the effective ranges r_ℓ extracted from the computed scattering amplitude.

Here, we regularize the divergences by cutting off all integrals over the wave vectors \mathbf{k} at the scale Λ . The limit $\Lambda \rightarrow \infty$ will be taken after expressing E_Ω computed in terms of a_ℓ and r_ℓ s (as in [13], the cancellation of the terms diverging as $\Lambda \rightarrow \infty$ will serve as a partial check of the correctness of the calculation). Thus, to obtain the complete correction $E_\Omega^{(2)}$ to the result (3), C_0 in $E_\Omega^{(1)}$ has to be expressed through a_0 up to one-loop order. The interaction (6) leads to two one-loop diagrams shown in Figs. 1 (a) and 1 (b), representing scattering of a -fermions on b -fermions. The second one vanishes, however, owing to the absence of antiparticles; moreover, it is easy to see that this interaction generates a whole class of diagrams shown in Fig. 1 (c) which can be easily taken into account. Evaluating them using the standard Feynman rules [16] with the propagators

$$\langle \text{void} | \text{T} \psi_{a/b}(t, \mathbf{x}) \psi_{a/b}^\dagger(t', \mathbf{x}') | \text{void} \rangle = \int \frac{d^3 \mathbf{k}}{(2\pi)^3} e^{i\mathbf{k} \cdot (\mathbf{x} - \mathbf{x}')} \int \frac{d\omega}{2\pi} \frac{i e^{-i\omega(t-t')}}{\omega - \omega_{\mathbf{k}}^{a/b} + i0},$$

one obtains for the scattering amplitude the expression³

$$f(k, \theta) = -\frac{m_{\text{red}}}{2\pi\hbar^2} C_0 \left\{ 1 + \left(\frac{C_0}{i\hbar} \right) \left(\frac{2m_{\text{red}}}{i\hbar} I_0 \right) + \left(\frac{C_0}{i\hbar} \right)^2 \left(\frac{2m_{\text{red}}}{i\hbar} I_0 \right)^2 + \dots \right\}, \quad (9)$$

² The symbol T of the chronological ordering should not be confused with T denoting time.

³ Upon integrating over frequencies with the help of the residue method, the denominators of the propagators neatly combine so that the result depends only on m_{red} .

where

$$I_0 = \int \frac{d^3\mathbf{q}}{(2\pi)^3} \frac{1}{\mathbf{q}^2 - \mathbf{k}^2 - i0}. \quad (10)$$

The amplitude (9), supplemented in general with (k -dependent) terms which come from diagrams generated by the other interactions (omitted in (2)) of the effective Hamiltonian should be matched onto the expansion (4).

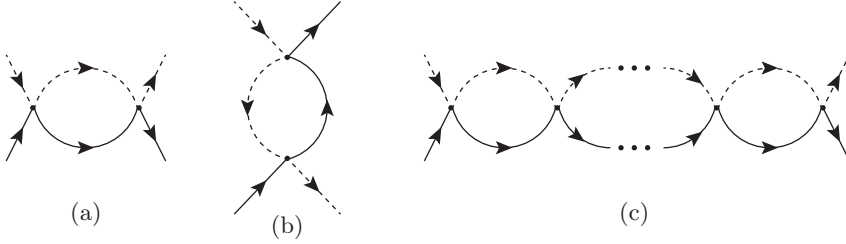


Fig. 1. Two one-loop Feynman diagrams representing the elastic scattering amplitude of the a -fermion (solid lines) on the b -fermion (dashed lines); the diagram (b) vanishes. The “sausage”-type diagrams (c) originating in higher orders from the interaction term proportional to C_0 . Time flows from the left to the right.

The integral I_0 is divergent and requires regularization. Imposing the UV cut-off Λ on $q = |\mathbf{q}|$, one obtains ($k = |\mathbf{k}|$)

$$\begin{aligned} I_0(k, \Lambda) &= \frac{1}{4\pi^2} \int_0^\Lambda dq q \left[\frac{1}{q - k - i0} + \frac{1}{q + k + i0} \right] \\ &= \frac{i}{4\pi} k + \frac{1}{2\pi^2} \Lambda - \frac{1}{2\pi^2} \frac{k^2}{\Lambda} + \dots, \end{aligned} \quad (11)$$

upon using the standard Sochocki formula $1/(x \pm i0) = P(1/x) \mp i\pi\delta(x)$ (P stands for principal value). Inserting this into formula (9) matched onto the expansion (4) and solving for C_0 , one finds

$$C_0 = \frac{2\pi\hbar^2}{m_{\text{red}}} a_0 \left(1 + \frac{2}{\pi} a_0 \Lambda + \dots \right). \quad (12)$$

The right-hand side of formula (8) can be evaluated using the standard rules of the many-body quantum field theory (see *e.g.* [16]). Because $|\Omega_0\rangle$ is the lowest energy state of N_a free a -fermions and N_b free b -fermions, in the momentum space lines of Feynman diagrams correspond to the propagators

$$i\tilde{G}_{a/b}^{(0)}(\omega, \mathbf{k}) = i \left[\frac{\theta(|\mathbf{k}| - p_{F_{a/b}})}{\omega - \omega_{\mathbf{k}}^{a/b} + i0} + \frac{\theta(p_{F_{a/b}} - |\mathbf{k}|)}{\omega - \omega_{\mathbf{k}}^{a/b} - i0} \right] \quad (13)$$

and, to account for the normal ordered form of the interaction term in (2), one has only to add the rule [16] that if a line originates from and ends up in one and the same vertex, the propagator (13) corresponding to this line has to be multiplied by $e^{i\omega\eta}$ with the limit of $\eta \rightarrow 0^+$ taken at the end.

In the first order in C_0 , there is only one connected vacuum graph shown in Fig. 2 which (evaluated in the position space) immediately gives $(iG_{a/b}^{(0)}(0))$ are the propagators (13) written in the position space)

$$TE_{\Omega}^{(1)} = C_0 VT iG_a^{(0)}(0) iG_a^{(0)}(0) = C_0 VT \frac{p_{Fa}^3}{6\pi^2} \frac{p_{Fb}^3}{6\pi^2},$$

which reproduces the result (3).

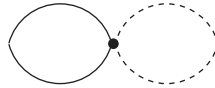


Fig. 2. The effective theory connected vacuum diagram of the order of C_0 reproducing the first-order correction $E_{\Omega}^{(1)}$. Solid and dashed lines represent propagators of a - and b -fermions, respectively.

As explained in [9], the only nonzero contribution to the second-order correction $E_{\Omega}^{(2)}$ comes from the Feynman diagram shown in Fig. 3. Performing the same steps as in the analogous computation [13] of the second-order correction to the ground-state energy of a polarized system of spin-1/2 fermions (to which the present computation reduces in the limit of $m_a = m_b$), one arrives at the expression

$$\begin{aligned} \frac{E_{\Omega}^{(2)}}{V} &= \frac{C_0^2}{\hbar} \int \frac{d^3\mathbf{q}}{(2\pi)^3} \int \frac{d^3\mathbf{p}}{(2\pi)^3} \\ &\times \int \frac{d^3\mathbf{k}}{(2\pi)^3} \frac{\theta(p_{Fa} - |\mathbf{k}|)\theta(p_{Fb} - |\mathbf{p}|)\theta(|\mathbf{k} + \mathbf{q}| - p_{Fa})\theta(|\mathbf{p} - \mathbf{q}| - p_{Fb})}{\omega_{\mathbf{k}}^a + \omega_{\mathbf{p}}^b - \omega_{\mathbf{k} + \mathbf{q}}^a - \omega_{\mathbf{p} - \mathbf{q}}^b + i0}. \end{aligned}$$

The next step is passing to the integrations over the variables \mathbf{s} , \mathbf{t} and \mathbf{u} defined by the relations (the Jacobian equals 8)

$$\mathbf{k} = \tilde{m}_a \mathbf{s} - \mathbf{t}, \quad \mathbf{p} = \tilde{m}_b \mathbf{s} + \mathbf{t}, \quad \mathbf{q} = \mathbf{t} - \mathbf{u},$$

which are the appropriate modification of those used in [9, 13], where

$$\tilde{m}_{a/b} = \frac{2m_{a/b}}{m_a + m_b}, \quad \tilde{m}_a + \tilde{m}_b = 2.$$

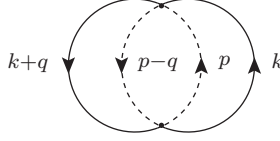


Fig. 3. The only nonvanishing three-loop connected vacuum diagram contributing the order $(k_f a_0)^2$ correction to the ground-state energy of the diluted gas of the mixture of (spin-1/2) a - and b -fermions. The two kinds of propagators differ by the values of the Fermi momenta; for definiteness, it is assumed that $p_{Fa} \geq p_{Fb}$.

The denominator of the integrand then becomes equal $\hbar(\mathbf{t}^2 - \mathbf{u}^2 + i0)/2m_{\text{red}}$ and the first- and second-order corrections to the ground-state energy can be, after using (12), written together in the form of

$$\frac{E_{\Omega}^{(1)} + E_{\Omega}^{(2)}}{V} = \frac{p_{Fb}^3 p_{Fa}^3}{9\pi^3} \frac{\hbar^2}{2m_{\text{red}}} a_0 + \frac{2p_{Fb}^3 p_{Fa}^3}{9\pi^4} \frac{\hbar^2}{2m_{\text{red}}} a_0^2 \Lambda + \frac{\hbar^2}{2m_{\text{red}}} 256 a_0^2 \frac{\tilde{J}}{(2\pi)^4}, \quad (14)$$

where $(\tilde{m}_b = 2 - \tilde{m}_a)$

$$\begin{aligned} \tilde{J}(p_{Fa}, p_{Fb}, \tilde{m}_a) &= \int_0^{s_{\text{max}}} ds s^2 \frac{1}{4\pi} \\ &\times \int d^3 t \theta(p_{Fb} - |\mathbf{t} + \tilde{m}_b \mathbf{s}|) \theta(p_{Fa} - |\mathbf{t} - \tilde{m}_a \mathbf{s}|) \tilde{g}(t, s), \\ \tilde{g}(t, s) \equiv \tilde{g}(|\mathbf{t}|, s) &= \frac{1}{4\pi} \int d^3 \mathbf{u} \frac{\theta(|\mathbf{u} + \tilde{m}_b \mathbf{s}| - p_{Fb}) \theta(|\mathbf{u} - \tilde{m}_a \mathbf{s}| - p_{Fa})}{t^2 - u^2 + i0}. \quad (15) \end{aligned}$$

The regions of the integrations over $d^3 \mathbf{u}$ and over $d^3 \mathbf{t}$ are determined by the intersections of two Fermi spheres of unequal radii, p_{Fb} and p_{Fa} , the centers of which are displaced from the origin of the \mathbf{u} (of the \mathbf{t}) space by the vectors $-\tilde{m}_b \mathbf{s}$ (\mathbf{s} will be taken to determine the z -axes of the \mathbf{u} and \mathbf{t} spaces in the integrals over $d^3 \mathbf{u}$ and $d^3 \mathbf{t}$) and $\tilde{m}_a \mathbf{s}$, respectively (the distance between the centers is $2|\mathbf{s}|$). This is the only modification compared to the computation done in [13]. The integral over \mathbf{u} runs over the infinite exterior of these spheres and is, therefore, divergent; the integration over \mathbf{t} covers the interior of their intersection. For this reason, the outermost integration over $s \equiv |\mathbf{s}|$ is restricted to $s \leq s_{\text{max}} = \frac{1}{2}(p_{Fa} + p_{Fb})$ because if $s > s_{\text{max}}$, the two spheres which determine the region of the integration over \mathbf{t} become disjoint.

As far as the integral giving $\tilde{g}(t, s)$ is concerned, the range of the variable s splits into two domains: $0 \leq s \leq s_0 = \frac{1}{2}(p_{Fa} - p_{Fb})$ and $s_0 \leq s \leq s_{\text{max}}$. Correspondingly, the integral \tilde{J} splits into $\tilde{J}_1 + \tilde{J}_2$.

If $0 \leq s \leq s_0$, the smaller sphere of radius p_{Fb} is entirely contained inside the one of radius p_{Fa} and plays no role in determining the domain of integration over \mathbf{u} : this domain is then just the (infinite) exterior of the sphere of radius p_{Fa} the center of which is at $u_z = 0$, when $s = 0$ and moves to the right as s increases. The computation of $\tilde{g}(t, s)$ for $0 \leq s \leq s_0$ and of \tilde{J}_1 proceeds, therefore, exactly as in the case of equal masses discussed in [13] and one readily finds that

$$\tilde{g}(t, s) = g(t, \tilde{m}_a s), \quad 0 \leq s \leq s_0, \quad (16)$$

where

$$\begin{aligned} g(t, s) = & -\Lambda + \frac{1}{2} p_{Fa} + \frac{t}{4} \ln \frac{(p_{Fa} - t)^2 - s^2}{(p_{Fa} + t)^2 - s^2} + \frac{p_{Fa}^2 - s^2 - t^2}{8s} \\ & \times \ln \frac{(p_{Fa} + s)^2 - t^2}{(p_{Fa} - s)^2 - t^2} \end{aligned} \quad (17)$$

is the function obtained in [13] in the case of $m_a = m_b$.

Since \tilde{J}_1 is obtained by integrating the function $\tilde{g}(t, s)$ first over the interior of the sphere of radius p_{Fb} , the center of which is shifted by $-\tilde{m}_b \mathbf{s}$ from the origin of the \mathbf{t} space, and then, with the weight s^2 , over s from 0 to s_0 , it is straightforward to obtain the divergent part \tilde{J}_1^{div} of \tilde{J}_1

$$\tilde{J}_1^{\text{div}} = -\frac{1}{9} \Lambda s_0^3 p_{Fb}^3 = -\frac{1}{72} \Lambda (p_{Fa} - p_{Fb})^3 p_{Fb}^3. \quad (18)$$

The finite part of \tilde{J}_1 can be easily obtained by numerical integration. This can be done either by writing $\mathbf{t} = \mathbf{t}' - \tilde{m}_b \mathbf{s}$ and introducing the spherical coordinate system in the \mathbf{t}' space with the t'_z axis taken in the direction of the vector \mathbf{s}

$$\tilde{J}_1 = \frac{1}{2} \int_0^{s_0} ds s^2 \int_{-1}^1 d\eta \int_0^{p_{Fb}} dt' t'^2 g \left(\sqrt{t'^2 - 2t'\tilde{m}_b s \eta + \tilde{m}_b^2 s^2}, \tilde{m}_a s \right),$$

or just by using the *Mathematica* instruction `0.5NIntegrate[s^2 t^2 g[t, \tilde{m}_a s] Boole[t^2 + 2t\tilde{m}_b s x + \tilde{m}_b^2 s^2 < p_{Fb}^2], {s, 0, s_0}, {x, -1, 1}, {t, 0, \infty}]`.

We now compute the function $\tilde{g}(t, s)$ for $s_0 \leq s \leq s_{\text{max}}$ and the corresponding contribution \tilde{J}_2 to the integral (15). In this regime, the two Fermi spheres which determine the ranges of integrations over \mathbf{u} and over \mathbf{t} intersect one another. In the \mathbf{u} space, the z coordinate u_z^0 of the intersection and its distance u_0 from the origin are determined by solving the equations

$$\begin{aligned} u_\perp^2 + (u_z - \tilde{m}_a s)^2 &= p_{Fa}^2, \\ u_\perp^2 + (u_z + \tilde{m}_b s)^2 &= p_{Fb}^2, \end{aligned}$$

which give (recall that $\tilde{m}_a + \tilde{m}_b = 2$)

$$\begin{aligned} u_z^0 &= -\frac{1}{4s} (p_{\text{F}a}^2 - p_{\text{F}b}^2) + \frac{1}{2} (\tilde{m}_a - \tilde{m}_b) s, \\ u_0^2 &= \frac{1}{2} (\tilde{m}_b p_{\text{F}a}^2 + \tilde{m}_a p_{\text{F}b}^2) - \tilde{m}_a \tilde{m}_b s^2. \end{aligned} \quad (19)$$

In the spherical system, the “critical” angles ϑ_0 corresponding to the intersection of the spheres (marked in Fig. 4) are given by

$$\cos \vartheta_0 = \xi_0 = \frac{u_z^0}{u_0}. \quad (20)$$

Therefore, if $s_0 \leq s \leq s_{\text{max}}$ (i.e. when the two Fermi spheres intersect), the function $\tilde{g}(t, s)$ is given by⁴

$$\tilde{g}(t, s) = \frac{1}{2} \int_{-1}^{\xi_0} d\xi \int_{u_b(\xi, s)}^{\Lambda} du \frac{u^2}{t^2 - u^2 + i0} + \frac{1}{2} \int_{\xi_0}^1 d\xi \int_{u_a(\xi, s)}^{\Lambda} du \frac{u^2}{t^2 - u^2 + i0}, \quad (21)$$

where

$$\begin{aligned} u_b(\xi, s) &= -\tilde{m}_b s \xi + \sqrt{p_{\text{F}b}^2 - \tilde{m}_b^2 s^2 (1 - \xi^2)}, \\ u_a(\xi, s) &= \tilde{m}_a s \xi + \sqrt{p_{\text{F}a}^2 - \tilde{m}_a^2 s^2 (1 - \xi^2)}; \end{aligned}$$

of course $u_b(\xi_0, s) = u_a(\xi_0, s) \equiv u_0$. After extracting the terms diverging with $\Lambda \rightarrow \infty$ as in [9, 13] (they combine to $-2\pi^2 I_0$, where I_0 is given in (11)), one gets

$$\begin{aligned} \tilde{g}(t, s) &= -\Lambda - i\frac{\pi}{2}t + \frac{1}{2} \int_{-1}^{\xi_0} d\xi \int_0^{u_b(\xi, s)} du \frac{u^2}{u^2 - t^2 - i0} \\ &\quad + \frac{1}{2} \int_{\xi_0}^1 d\xi \int_0^{u_a(\xi, s)} du \frac{u^2}{u^2 - t^2 - i0}. \end{aligned}$$

⁴ Actually, this way of computing $\tilde{g}(t, s)$ in this regime ($s_0 < s < s_{\text{max}}$) is justified geometrically only for s not greater than some critical value (depending on the ratios $p_{\text{F}b}/p_{\text{F}a}$ and m_b/m_a) which is smaller than s_{max} . For s greater than critical, the dashed lines in Fig. 4 pass through the interiors of the smaller spheres and formula (21) may seem to be unjustified. We have checked, however, by integrating numerically functions over the domain formed by the exterior of the intersecting spheres lying inside a large sphere of radius $R > 2p_{\text{F}a}$ that formula (21) always gives the correct answer.

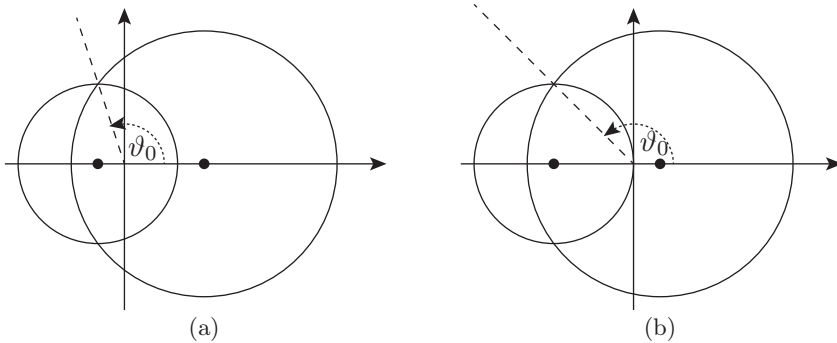


Fig. 4. Intersecting Fermi spheres for $(p_{Fa} - p_{Fb})/2 < s < (p_{Fa} + p_{Fb})/2$. Dots mark their centers shifted by $-\tilde{m}_b s$ and $\tilde{m}_a s$ from the origin of the space. (a) $m_a > m_b$, (b) $m_a < m_b$. Marked are the “critical” polar angles ϑ_0 .

It is now straightforward to compute \tilde{J}_2^{div} and to check the cancellation of Λ . Indeed, the integral

$$\frac{1}{4\pi} \int d^3\mathbf{t} \theta(p_{Fb} - |\mathbf{t} + \tilde{m}_b \mathbf{s}|) \theta(p_{Fa} - |\mathbf{t} - \tilde{m}_a \mathbf{s}|) (-\Lambda)$$

can be done by shifting the origin of the \mathbf{t} space so that the intersection of the two Fermi spheres occurs at $t'_z = 0$. The integration over $d^3\mathbf{t}$ is then easy and its result is

$$-\frac{\Lambda}{2} \left\{ \left[\frac{1}{3} p_{Fb}^3 - \frac{1}{2} p_{Fb}^2 (s + u_z^0) + \frac{1}{6} (s + u_z^0)^3 \right] + \left[\frac{1}{3} p_{Fa}^3 - \frac{1}{2} p_{Fa}^2 (s - u_z^0) + \frac{1}{6} (s - u_z^0)^3 \right] \right\},$$

where u_z^0 is given by (19). This should be integrated from $s_0 = \frac{1}{2}(p_{Fa} - p_{Fb})$ to $s_{\text{max}} = \frac{1}{2}(p_{Fa} + p_{Fb})$ with the weight s^2 . Mathematica does the integration readily with the expected result

$$\tilde{J}_2^{\text{div}} = -\Lambda \left(\frac{p_{Fa}^2 p_{Fb}^4}{24} - \frac{p_{Fa} p_{Fb}^5}{24} + \frac{p_{Fb}^6}{72} \right).$$

Combining this with the divergent part (18) of \tilde{J}_1 , one gets

$$\tilde{J}_1^{\text{div}} + \tilde{J}_2^{\text{div}} = -\Lambda \frac{p_{Fb}^3 p_{Fa}^3}{72},$$

which is precisely what is needed to cancel in (14) the term explicitly proportional to Λ which comes from expressing C_0 in terms of the scattering length in the first order result.

The remaining integrals in $\tilde{g}(t, s)$ can be worked out exactly as in [13] using the trick given in Appendix C of [15], that is by taking the integrals over ξ by parts after inserting into them $1 = d\xi/d\xi$. The integrals have imaginary parts which together precisely cancel the imaginary part which arose from the divergent integral I_0 and the final result for $s_0 \leq s \leq s_{\max}$ is

$$\begin{aligned} \tilde{g}(t, s) = & -\Lambda + \frac{1}{4}(p_{Fb} + p_{Fa} + 2s) + \frac{t}{4} \ln \frac{p_{Fb} + \tilde{m}_b s - t}{p_{Fb} + \tilde{m}_b s + t} + \frac{t}{4} \ln \frac{p_{Fa} + \tilde{m}_a s - t}{p_{Fa} + \tilde{m}_a s + t} \\ & + \frac{p_{Fb}^2 - t^2 - \tilde{m}_b^2 s^2}{8\tilde{m}_b s} \ln \frac{(p_{Fb} + \tilde{m}_b s)^2 - t^2}{u_0^2 - t^2} \\ & + \frac{p_{Fa}^2 - t^2 - \tilde{m}_a^2 s^2}{8\tilde{m}_a s} \ln \frac{(p_{Fa} + \tilde{m}_a s)^2 - t^2}{u_0^2 - t^2}, \end{aligned} \quad (22)$$

where u_0^2 is given in (19). In the limit of $m_a = m_b$ (*i.e.* $\tilde{m}_a = \tilde{m}_b = 1$), the results (16) and (22) go over into the ones obtained in [13] which agree with the result obtained in [14]. The finite parts of the functions \tilde{J}_1 and \tilde{J}_2 , *i.e.* the integrals over t , η , and s , can be easily evaluated using, for instance, the standard **Mathematica** function allowing to numerically perform integrations over (multidimensional) domains. Since the finite part of $\tilde{J} = \tilde{J}_1 + \tilde{J}_2$ scales as the seventh power of p_{Fa} , in Fig. 5 we show $\tilde{J}(r, 1, \tilde{m}_a)$ as a function of $r = p_{Fb}/p_{Fa}$ for several values of the mass ratio m_b/m_a . It is clear that the curves corresponding to $m_b/m_a = x$ and $1/x$ merge for $r = 1$

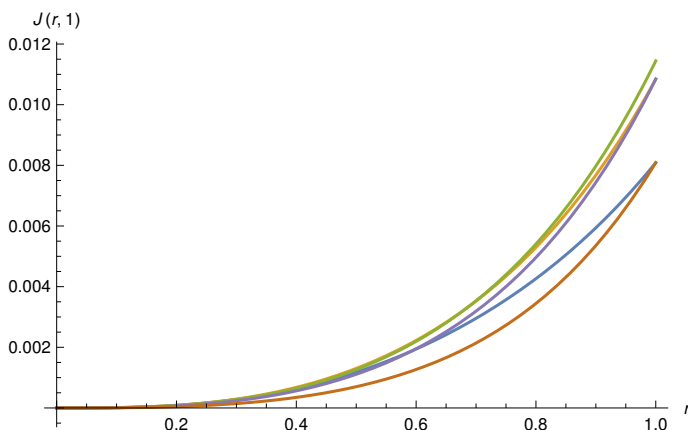


Fig. 5. The plot of the function $\tilde{J}(r, 1, \tilde{m}_a)$. The consecutive lines (counting from below at $r \sim 0.9$) correspond to the ratio m_b/m_a equal to 40/6 (red), 6/40 (blue), 2 (violet), 1/2 (yellow), and 1 (green). At $r = 1$ (zero polarization), the results for $m_b/m_a = x$ and $m_b/m_a = 1/x$ coincide as they should. The value $\tilde{J}(1, 1, 1) = 0.0114449 = (11 - 2 \ln 2)/840$ (the endpoint of the green curve for $m_b/m_a = 1$) is the the result of [9].

(vanishing polarization) as they should; also, independently of the mass ratio, the function \tilde{J} vanishes for the maximal polarization (at $P = 1$, *i.e.* for $r = 0$) when all fermions are of the same type, as required by the Pauli exclusion principle.

3. Results

The energy density with the order $(k_F a_0)^2$ term included can be expressed in several equivalent ways. Either in terms of the ratio $r \equiv p_{Fb}/p_{Fa}$ and $k_F \equiv 3\pi^2(N_a + N_b)/V$, so that $p_{Fa} = k_F(2/(1+r^3))^{1/3}$,

$$\begin{aligned} \frac{E_\Omega}{V} = & \frac{k_F^3}{3\pi^2} \frac{\hbar^2 k_F^2}{4m_{\text{red}}} \left(\frac{2}{1+r^3} \right)^{5/3} \left\{ \frac{3}{10} (\tilde{m}_b + \tilde{m}_a r^5) + \frac{2}{3\pi} r^3 \left(\frac{2}{1+r^3} \right)^{1/3} (k_F a_0) \right. \\ & \left. + \frac{96}{\pi^2} \left(\frac{2}{1+r^3} \right)^{2/3} (k_F a_0)^2 \tilde{J}(1, r, \tilde{m}_a) + \dots \right\}, \end{aligned} \quad (23)$$

or in terms of the polarization $P = (N_a - N_b)/(N_a + N_b) = (1 - r^3)/(1 + r^3)$

$$\begin{aligned} \frac{E_\Omega}{V} = & \frac{k_F^3}{3\pi^2} \frac{\hbar^2 k_F^2}{4m_{\text{red}}} \left\{ \frac{3}{10} (\tilde{m}_b(1+P)^{5/3} + \tilde{m}_a(1-P)^{5/3}) + \frac{2}{3\pi} (1 - P^2) (k_F a_0) \right. \\ & \left. + \frac{96}{\pi^2} (1 + P)^{7/3} (k_F a_0)^2 \tilde{J}(1, r(P), \tilde{m}_a) + \dots \right\}, \end{aligned} \quad (24)$$

where $r(P) = ((1 - P)/(1 + P))^{1/3}$. Note also that the prefactor $\hbar^2 k_F^5 / 12\pi^2 m_{\text{red}}$ in this formula can be written in the form of

$$(N/V)(\hbar^2 k_F^2 / 4m_{\text{red}}).$$

At zero polarization ($r = 1$, $P = 0$), formula (24) simplifies to

$$\frac{E_\Omega}{V} = \frac{k_F^3}{3\pi^2} \frac{\hbar^2 k_F^2}{4m_{\text{red}}} \frac{3}{5} \left\{ 1 + \frac{10}{9\pi} (k_F a_0) + \frac{160}{\pi^2} (k_F a_0)^2 \tilde{J}(1, 1, \tilde{m}_a) + \dots \right\}. \quad (25)$$

Setting here $\tilde{m}_a = 40/23$, *i.e.* $m_b/m_a = 6/40$, one finds that with $\tilde{J} = 0.00808856$, this agrees with the second-order result shown for this mass ratio in Fig. 1 of [1]. No plots of energy density for nonzero polarization are shown in [1] but the authors give an interpolation formula for the evaluated numerically function $I(P, m_b/m_a)$ in terms of which their second-order correction to the system's energy is expressed. The precise relation of this function I to our function \tilde{J} should be

$$\begin{aligned} & \frac{m_a + m_b}{m_b} I(P, m_b/m_a) \\ & = 320(1 + P)^{7/3} \tilde{J} \left(1, ((1 - P)/(1 + P))^{1/3}, 2m_a/(m_a + m_b) \right). \end{aligned}$$

We have checked that although the interpolation formula of [1] yields for $P = 1$ a small but nonzero value of the function I (slightly at variance with the Pauli exclusion principle), it nevertheless agrees excellently with the results of our calculation.

The energy density given by formula (24) in the case of equal masses ($m_a = m_b \equiv m_f$) of the oppositely polarized fermions is shown in Fig. 6. It illustrates the well-known fact [19] that the emergence of a nonzero polarization (of the global minimum of the energy density as a function of P) which in the mean-field approximation (*i.e.* with only the order $k_F a_0$ term included) is a second-order transition [4], after the inclusion of the second-order term becomes the first-order one. This, however, occurs probably beyond the limits of the reliability of the approximation used: for vanishing polarization, the comparison of the second-order formula with the results of the quantum Monte Carlo simulations of [6] shows that it is numerically reliable only up to $k_F a_0 \lesssim 0.5$.

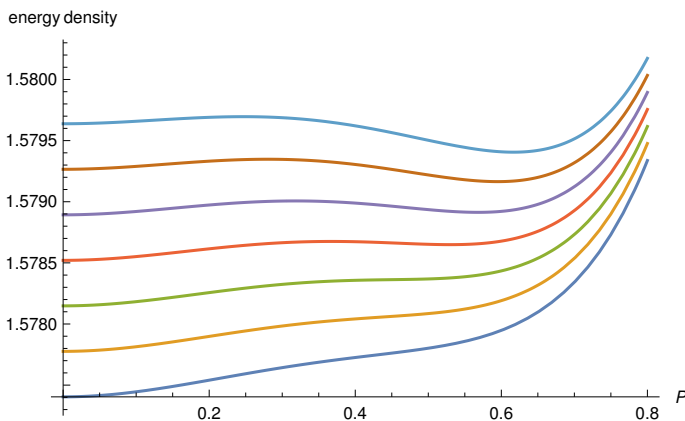


Fig. 6. Energy density E_{Ω}/V in units $(3/5)(\hbar^2 k_F^2/2m_f)(k_F^3/3\pi^2)$ of the gas of the same mass ($m_a = m_b \equiv m_f$) spin-1/2 fermions as a function of the polarization P for different values (from below): 1.0520 (blue), 1.0525 (yellow), 1.0530 (green), 1.0535 (red), 1.0540 (violet), 1.0545 (dark red), and 1.0550 (light blue) of $k_F a_0$. The emergence of the ferromagnetic behaviour as well as the first-order character of the transition to the ferromagnetic state are clearly seen.

If the masses of oppositely polarized fermions differ, the minimum of the energy density is at $P \neq 0$ already in the case of vanishing interactions (the system is polarized in the direction of the polarization of the heavier species). If the mass ratio corresponds to different atoms, this effect completely dominates the dependence of the energy density on the polarization. Only if the mass ratio is very close to unity (as would be if different isotopes of the same element could play the roles two different fermion species), can

the mean-field correction generate a higher (*i.e.* unstable), second minimum at an opposite polarization and this only when $k_F a_0 \approx \pi/2$; for such strengths of the interaction, however, the second-order correction computed in this paper and in [1] is so large, that the two minima (the deeper one corresponding to the direction of the polarization of heavier isotopes) occur already at $P = \pm 1$ and the discussion of the change of the order of the transition is meaningless in view of the clear unreliability of the expansion. In Fig. 7, the effects of inclusion of the second-order term in the case of the mass ratio $m_b/m_a = 2/3$ are shown for $k_F a_0 = 0.5$ to show that when the expansion is reliable, the minimum of the energy density at a nonzero polarization, existing already without any interaction, can only be slightly displaced.

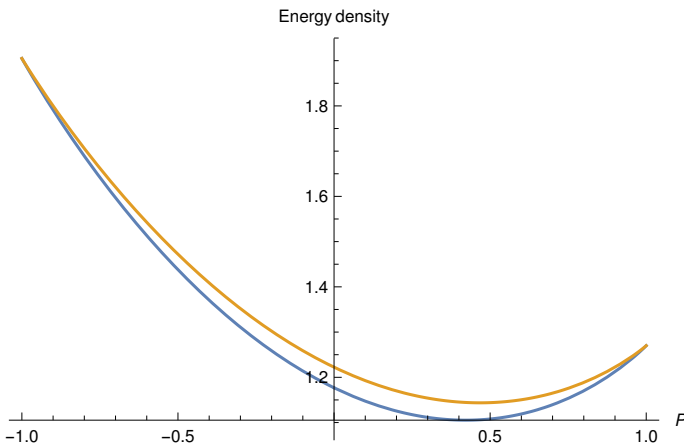


Fig. 7. Energy density E_Ω/V in units $(3/5)(\hbar^2 k_F^2/4m_{\text{red}})(k_F^3/3\pi^2)$ of the mixture of two species of oppositely polarized spin-1/2 fermions with the mass ratio $m_b/m_a = 2/3$ and $k_F a_0 = 0.5$, as a function of the polarization P . The lower curve is the mean-field result, while the upper one shows the effects of inclusion the term of the order of $(k_F a_0)^2$.

4. Final remarks

We have shown that the order $(k_F a_0)^2$, where a_0 is the *s*-wave scattering length and $k_F = (3\pi^2 N/V)^{1/3}$, correction to the ground-state energy of a mixture of the oppositely polarized fermions of different masses, computed for the first time in [1] by using a complicated numerical evaluation of the formulae derived in [8], can be easily and semi-analytically reproduced in the effective theory approach proposed first in [9] which is simple and leads to integrals which can be numerically evaluated using the standard built-in Mathematica routines. Thus, this method can allow for extending the computation to yet higher orders.

We would like to thank Sebastiano Pilati and the anonymous referee of paper [13] for suggesting us this extension of the method.

REFERENCES

- [1] E. Fratini, S. Pilati, «Zero-temperature equation of state and phase diagram of repulsive fermionic mixtures», *Phys. Rev. A* **90**, 023605 (2014).
- [2] G.-B. Jo *et al.*, «Itinerant Ferromagnetism in a Fermi Gas of Ultracold Atoms», *Science* **325**, 1521 (2009).
- [3] Y.-R. Lee *et al.*, «Compressibility of an ultracold Fermi gas with repulsive interactions», *Phys. Rev. A* **85**, 063615 (2012); C. Sanner *et al.*, «Correlations and Pair Formation in a Repulsively Interacting Fermi Gas», *Phys. Rev. Lett.* **108**, 240404 (2012).
- [4] E. Stoner, «LXXX. Atomic moments in ferromagnetic metals and alloys with non-ferromagnetic elements», *Philos. Mag.* **15**, 1018 (1933); see also Section 13.4 in: K. Huang, «Statistical Mechanics», *John Willey and Sons, Inc.*, New York 1963.
- [5] G.J. Conduit, A.G. Green, B.D. Simons, «Inhomogeneous Phase Formation on the Border of Itinerant Ferromagnetism», *Phys. Rev. Lett.* **103**, 207201 (2009); S.-Y. Chang, M. Randeria, N. Trivedi, «Ferromagnetism in the upper branch of the Feshbach resonance and the hard-sphere Fermi gas», *Proc. Natl. Acad. Sci. USA* **108**, 51 (2011).
- [6] S. Pilati, G. Bertaina, S. Giorgini, M. Troyer, «Itinerant Ferromagnetism of a Repulsive Atomic Fermi Gas: A Quantum Monte Carlo Study», *Phys. Rev. Lett.* **105**, 030405 (2010), [arXiv:1004.1169 \[cond-mat.quant-gas\]](https://arxiv.org/abs/1004.1169).
- [7] D. Pekker *et al.*, «Competition between Pairing and Ferromagnetic Instabilities in Ultracold Fermi Gases near Feshbach Resonances», *Phys. Rev. Lett.* **106**, 050402 (2011).
- [8] A.A. Abrikosov, L.P. Gorkov, I.E. Dzialoshinski, «Methods of Quantum Field Theory in Statistical Physics», *Dover Publications, Inc.*, New York 1975.
- [9] H.-W. Hammer, R.J. Furnstahl, «Effective field theory for dilute Fermi systems», *Nucl. Phys. A* **678**, 277 (2000), [arXiv:nuc1-th/0004043](https://arxiv.org/abs/nuc1-th/0004043).
- [10] H.-W. Hammer, S. König, U. van Kolck, «Nuclear effective field theory: Status and perspectives», *Rev. Mod. Phys.* **92**, 025004 (2020).
- [11] See *e.g.* R. Seki, U. van Kolck, M. Savage (Eds.) «Proceedings of the Joint Caltech/INT Workshop *Nuclear Physics with Effective Field Theory*», *World Scientific*, 1998; P.F. Bedaque, M. Savage, R. Seki, U. van Kolck (Eds.) «Proceedings of the INT Workshop *Nuclear Physics with Effective Field Theory II*», *World Scientific*, 2000.
- [12] C. Wellenhofer, C. Drischler, A. Schwenk, «Dilute Fermi gas at fourth order in effective field theory», *Phys. Lett. B* **802**, 135247 (2020).
- [13] P. Chankowski, J. Wojtkiewicz, «Ground-state energy of the polarized dilute gas of interacting spin- $\frac{1}{2}$ fermions», *Phys. Rev. B* **104**, 144425 (2021).

- [14] S. Kanno, «Criterion for the Ferromagnetism of Hard Sphere Fermi Liquid. II», *Prog. Theor. Phys.* **44**, 813 (1970).
- [15] R.J. Furnstahl, H.-W. Hammer, N. Tirfessa, «Field redefinitions at finite density», *Nucl. Phys. A* **689**, 846 (2001).
- [16] A.L. Fetter, J.D. Walecka, «Quantum Theory of Many Particle Systems», *McGraw Hill*, 1971.
- [17] R.P. Feynman, «Statistical Mechanics. A Set of Lectures», *W.A. Benjamin, Inc.*, 1972.
- [18] S. Weinberg, «The Quantum Theory of Fields. Vol. I», *Cambridge University Press*, 1995.
- [19] R.A. Duine, A.H. MacDonald, «Itinerant Ferromagnetism in an Ultracold Atom Fermi Gas», *Phys. Rev. Lett.* **95**, 230403 (2005).